Contributions of CO_2, O_2 and H_2O to the Oxidative Stability of Solid Amine Direct Air Capture Sorbents at Intermediate Temperature

Yoseph A. Guta,[1] Juliana Carneiro,[1] Sichi Li,[2] Giada Innocenti,[1] Simon H. Pang,[2] Miles A. Sakwa-Novak,[3] Carsten Sievers,[1]* Christopher W. Jones[1]*

[1]School of Chemical & Biomolecular Engineering, Georgia Institute of Technology, 311 Ferst Dr., Atlanta, GA 30332, United States
[2]Lawrence Livermore National Laboratory, 7000 East Avenue, Livermore, CA 94550, United States
[3]Global Thermostat, 10275 E106th Ave, Brighton, CO 80601, United States

*Corresponding authors: cjones@chbe.gatech.edu: carsten.sievers@chbe.gatech.edu

Abstract

Aminopolymer-based sorbents are preferred materials for extraction of CO_2 from ambient air (direct air capture of CO_2, or DAC) owing to their high CO_2 adsorption capacity and selectivity at ultra dilute conditions. While those adsorptive properties are important, the stability of a sorbent is a key element in developing high-performing, cost-effective, and long-lasting sorbents that can be deployed at scale. Along with process upsets, environmental components such as CO_2, O_2, and H_2O may contribute to long-term sorbent instability. As such, unraveling the complex effects of such atmospheric components on sorbent lifetime as they appear in the environment is a critical step to understanding sorbent deactivation mechanisms and designing more effective sorbents and processes. Here, PEI/Al_2O_3 sorbent is assessed over continuous and cyclic dry and humid conditions to determine the effect of the co-presence of CO_2 and O_2 on stability at an intermediate temperature of 70 °C. Thermogravimetric and elemental analysis in combination with *in situ* HATR-IR spectroscopy are performed to measure the extent of deactivation, elemental content, and molecular level changes in the sorbent due to deactivation. The thermal/thermogravimetric analysis results reveal that incorporating CO_2 with O_2 accelerates sorbent deactivation using these sorbents in dry and humid conditions compared to CO_2-free air in similar conditions. *In situ* HATR-IR spectroscopy results of PEI deactivation under a CO_2-air environment show the formation of primary amine species in higher quantity (compared to conditions without O_2 or CO_2), which arise due to C-N bond cleavage at the primary and secondary amine due to oxidative degradation. We hypothesize the formation of bound CO_2 species such as carbamic acids catalyze C-N cleavage reactions in the oxidative degradation pathway by shuttling protons, resulting in a lower activation energy barrier for degradation, as probed by metadynamics simulations. In the cyclic experiment after 30 cycles, results show a gradual loss in stability (dry: 29%, humid: 52%) under CO_2 containing air (0.04% CO_2/21% O_2 balance N_2). However, the loss in capacity during cyclic studies is significantly less than continuous deactivation as expected.

Keywords:

DAC, carbon capture, degradation, poly(ethylene imine), PEI, oxidation, radical

Introduction

Global greenhouse gas (GHG) emissions from various economic sectors have been growing rapidly for several decades.[1] GHGs present in the atmosphere absorb and retain heat released from Earth increasing the global surface temperature, warming oceans, melting of arctic ice, and causing sea level rise. CO_2 emissions, which were 80% of the released GHGs in 2019, have increased the atmospheric CO_2 concentration from 331 ppm (1975) to 416 ppm (current), raising the global average surface temperature by nearly 1°C.[1] Maintaining the current GHG emissions profile will lead to an increase of the global surface temperature by more than 1.5°C in the near future.[1, 2] Therefore, it is essential to develop robust technologies to limit the future emissions of GHGs and reverse the already existing damage.

Direct air capture (DAC) technologies for the removal of CO_2 from the atmosphere (negative emissions) and carbon capture technologies for large point sources (avoided emissions) such as coal-fired power plants are proposed technologies to address continuously increasing greenhouse gas emissions.[3] Considering the large amount of CO_2 present in the atmosphere and the goal of limiting the global surface temperature increase below 2 °C, quickly developing and deploying DAC processes, alongside other negative emissions technologies,[4] is important to climate stabilization. To this end, developing practical sorbent materials with high CO_2 selectivity, adsorption capacity and cyclic stability is necessary.[1, 5, 6]

Amine-functionalized sorbents are components of promising DAC technologies that are in the early stages of commercialization due to their high CO_2 selectivity, moderate regeneration energies, high CO_2 adsorption capacities and capability to perform under dry and humid conditions.[7, 8] Poly(ethylenimine) (PEI) supported in porous γ-Al_2O_3 (PEI/γ-Al_2O_3) is a well-known and well-studied supported aminopolymer sorbent in the DAC literature and is the focus of this study.[7, 9] One drawback of amine functionalized adsorbents is their susceptibility to loss of their high CO_2 adsorption capacity when operating continuously over multiple adsorption/desorption cycles in DAC systems. In a typical DAC adsorption/desorption cycle, sorbents are exposed to ambient air composed of several components such as O_2, CO_2, N_2, H_2O, and other small atmospheric molecules and particles. These components together with varying process parameters during different parts of the cycle (temperature, pressure, etc.) affect the long-term sorbent stability in a complex way.[10-14] One main example of this is the co-presence of high O_2 concentration (~21 mol%) and elevated temperatures associated with sorbent regeneration for short periods of time, which is considered to be the primary opportunity for oxidative degradation. The presence of other components of ambient air such as CO_2 and H_2O, in addition to the elevated O_2 concentration, alongside constantly changing process conditions, leads to an array of factors that may affect the sorbent's oxidative degradation behavior, mechanism(s), and the resulting longevity of the sorbent.

Studies of materials and processes for DAC to date have mostly focused on improving CO_2 adsorption capacities of solid sorbents. While adsorption capacity is an important factor, several studies have indicated that a sorbent material that can be used for thousands of adsorption/desorption cycles would substantially reduce overall DAC technology costs.[9] Of the studies on sorbent deactivation to date, most have focused on investigating the effects of exposure to O_2, H_2O, or CO_2 at elevated temperatures.[15-18] Furthermore, high temperatures that may not be directly relevant to the process are often used to accelerate the deactivation kinetics. The most explored deactivation paths include CO_2-induced deactivation and oxidative degradation in the presence of simulated air (21% O_2 balance N_2, dry, CO_2-free). In 2012, Heydari-Gorji et al.[10] investigated thermal, oxidative, and CO_2-induced deactivation of poly(ethylenimine)(PEI)-impregnated mesoporous silica (SBA-15) with platelet particle morphology and short pore channels under inert gas, simulated air, simulated flue gas and various $CO_2/O_2/N_2$ conditions. They found that the presence of humidity helped mitigate CO_2-induced deactivation using a 5% CO_2/N_2 mixture. Similarly, in pre-humidified $CO_2/O_2/N_2$ mixtures, they observed improved sorbent stability, suggesting that CO_2 and/or H_2O protected them against oxidative degradation.[10] In a follow up work by the same group, CO_2-induced deactivation under dry cyclic conditions using a flow of pure CO_2 both for adsorption at 50 °C or 100 °C and desorption at 130 °C-160 °C was explored.[11] Several amine-grafted MCM-41 and wet impregnated PEI (branched and linear) mesoporous silica sorbents were explored to understand the reaction mechanism(s) and products formed. Both studies suggested urea formation as a result of CO_2-induced deactivation at elevated temperatures and atmospheric pressure. As such, reaction pathways for open chain and cyclic urea formation were explored by others.[10, 11] Didas et al. explored the thermal,

oxidative, and CO_2-induced deactivation of primary amine grafted mesoporous silica (SBA-15) adsorbents with alkyl linker lengths varying from methyl to propyl under pure CO_2 at 135 °C. Ethyl and propyl linkers showed better resistance to oxidative and thermal deactivation; both, however, were vulnerable to CO_2 induced deactivation.[12]

While these studies helped build foundational knowledge of sorbent deactivation, mainly on CO_2-induced deactivation, they mostly explored flue gas CO_2 capture conditions where the CO_2, H_2O and O_2 concentrations differ from direct air capture. As such, the roles of CO_2, H_2O, and O_2 in sorbent stability might not be directly transferable to DAC conditions where the concentrations are different and temperatures are lower. Notably, a recent study from our group on the impact of atmospheric humidity on the stability of PEI/Al_2O_3 sorbent showed that H_2O plays a significant role in accelerating degradation reactions on some sorbents, which is contrary to the other reports in literature as briefly mentioned above.[17] To this end, a broad understanding of the impact of ambient air components ($H_2O/CO_2/O_2/N_2$) as they appear in the environment needs in depth exploration. A coherent and fundamental understanding of the deactivation mechanisms and behaviors is critical to the development of sorbent materials with significantly improved stability, reducing the cost of DAC. Furthermore, utilizing exemplar mixtures used in practical DAC applications allows for the accelerated implementation.[19]

In this work, we investigate environmental parameters that influence sorbent stability that have not been fully explored in the DAC literature. Specifically, we assess the impact of incorporating dry and humid CO_2 in air on the stability of a model aminopolymer sorbent (PEI/Al_2O_3) and its influence on the oxidative degradation behavior at intermediate temperatures (70 °C) directly relevant to the CO_2 desorption process. Furthermore, we explore the effect of humidity on sorbent stability in the presence and absence of CO_2 at the same temperature. *In situ* and *ex situ* spectroscopic, thermal, and elemental characterization of pristine and oxidized sorbents is performed using ATR-IR spectroscopy, alongside thermal analysis via thermogravimetric analysis to achieve the experimental goals. Metadynamics simulations are performed to gain further insight into the role of CO_2 during oxidation degradation. The knowledge gained from this study will enable further identification of aminopolymer sorbent deactivation pathways and products.

Experimental Methods

Materials & Sorbent Synthesis

Aminopolymer sorbents were synthesized by wet impregnation of PEI (branched, 800 g/mol, Sigma-Aldrich) onto a mesoporous gamma-alumina (Catalox HP 14/15 γ-Al_2O_3, Sasol) support (surface area 136 m^2/g and pore volume 0.95±0.05 cm^3/g). Branched PEI (without γ-Al_2O_3) was used for infrared spectroscopic analysis studies while 45 wt.% PEI/ γ-Al_2O_3 sorbent was used for thermal analysis studies.

N_2 physisorption was used to characterize the pore volume and pore size of the sorbent (PEI/ γ-Al_2O_3) and the support (γ-Al_2O_3). N_2 Physisorption was performed on Micromeritics TriStar II 3020 Version 3.02 at 77 K using 100 – 150 mg of sorbent. The samples were pretreated under vacuum at 100 °C for 10 h prior to the adsorption measurement. The pore size distribution was calculated using the Barrett-Joyner-Halenda (BJH) method.[20]

Elemental analysis of the fresh and deactivated sorbents was carried out by Atlantic Microlabs to determine the CHN content of the samples before and after various treatments. Specifically, C/N, and H/(C+N) ratios were calculated to understand the evolution of the elemental composition as the sorbent deactivates.

Thermogravimetric Combustion Analysis was used to determine the total organic content (PEI) of the sorbent. Organic combustion analysis was performed on a TGA (TA Instrument Q550) by heating the sample from room temperature to 700 °C with a ramp rate of 10 °C/min under Air (Airgas, UZG UZ300, 21% O_2 balance N_2). The weight loss of the sorbent from 160 °C to 700 °C was taken as the organic content.

CO_2 Adsorption Experiments

CO_2 adsorption experiments were conducted using a TGA (TA Instruments Q500) with 22 ±0.2 mg sample on a 50 μL platinum pan to investigate the CO_2 adsorption capacity. To pretreat the sample, He (Airgas UHP300) gas at 90 mL/min was flowed and the temperature was increased to 100 °C from room temperature at a ramp rate 10 °C/min and maintained for 1 h. Then, the temperature was lowered to 30 °C at a ramp rate of 10 °C/min. Once the system equilibrated at 30 °C, the gas was switched to 400 ppm CO_2 (balance He) at the same flow rate and held for 3 hours to allow for CO_2 adsorption. After 3 h of adsorption, the gas was switched back to He (Airgas UHP300) at 90 mL/min and the temperature was increased to 100 °C at a ramp rate of 10 °C/min to desorb the CO_2. The temperature was held

at 100 °C for 1 h to allow complete desorption of CO_2. At the end of the desorption, the temperature was reduced to 30 °C at a ramp rate of 10 °C/min to cool the instrument and prepare for the next run.

Thermal Analysis Experiments

Oxidation experiments were performed using a TGA-DSC (TA Instruments Q600) at 70 °C and 1 atm using 28±0.3 mg of sorbents (45% PEI/γ-Al_2O_3) on a 40 μL alumina ceramic pan. Prior to performing the deactivation study, the sample was purged with N_2 (Airgas UHP 99.999%) at flow rate of 100 mL/min at room temperature for 25 min followed by pretreatment at 100 °C for 1 h to remove adsorbed moisture and CO_2. After pretreatment, the temperature was reduced to 70 °C at a ramp rate of 5 °C per minute. Then, the temperature was held at 70 °C (isothermal) and the gas was switched to air (Airgas, UZG UZ300, 21% O_2 balance N_2) (CO_2-free air), 0.04% CO_2/21% O_2 balance N_2 (0.04% CO_2-air), or 0.04% CO_2 balance N_2 (0.04% CO_2-N_2) at 100 mL/min for the specified period of deactivation. For humid deactivation experiments, the deactivating gases were pre-humidified by flowing through a saturated K_2CO_3 solution at a temperature of 23°C, which provides ~43% relative humidity (RH). The relative humidity of the gas stream was monitored using a LI-COR 850 H_2O/CO_2 analyzer and was constant throughout the experiment. When the deactivation experiment was completed, the gas was switched back to N_2 and the temperature was lowered to 25 °C to limit further deactivation of the sorbent.

In situ ATR-IR spectroscopy

In situ IR experiments were conducted using Themo Scientific Nicolet 8700 HATR-IR (horizontal attenuated total reflection infrared) spectrometer with a ZnSe crystal cell to observe the effect of oxidation on fresh PEI (with no γ-Al_2O_3 support), tracking functional group formation due the various thermal treatments. For each experiment, about 0.1 mm PEI layer was coated on a ZnSe crystal and pretreated at 100 °C for 1 h under N_2 (Airgas UHP 99.999%) at 100 mL/min. Afterwards, the PEI was exposed to continuous flow of deactivating gas (simulated air (Airgas UZG UZ300, 21% O_2 balance N_2), 0.04% CO_2/21% O_2 balance N_2, or 0.04% CO_2 balance N_2) at 100 mL/min while the cell temperature was held at 70°C for 7 days. The HATR-IR spectra shown in this study were produced by subtraction of the spectrum of fresh PEI at 70 °C under the respective gas mixtures. As such, the spectra shown in the figures (with both positive and negative bands) are a result of changes in the sample due to exposure to the experimental conditions. A period of 7 days of deactivation was chosen based on the sorbent deactivation data obtained from the thermal analysis study. A peak deconvolution feature of Origin Pro 2021 was used to deconvolute peaks collected from the *in situ* ATR-IR experiments that are of interest and overlap with each other. The app used a built-in Gaussian function to perform the peak analysis.

First-principles metadynamics simulations

Ab initio molecular dynamics (AIMD) and metadynamics simulations were performed with the Vienna ab initio simulation package (VASP), version 5.4.4,[21] using the projector augmented wave treatment of core-valence interactions[22, 23] with the Perdew-Burke-Ernzerhof (PBE) generalized gradient approximation[24] for the exchange-correlation energy. DFT-D3 method of Grimme et al. was employed for vdW-dispersion energy corrections.[25] Triethylenetetramine (TETA) was used in all simulations as a small molecule surrogate for PEI. A 15 Å × 15 Å × 15 Å cubic supercell was used to accommodate TETA and CO_2-bound TETA molecules and the Brillouin zone was sampled at the Γ-point only. 10 ps of NVT AIMD simulations at 343 K were run to pre-equilibrate structures before initiating metadynamics simulations. Coordination numbers as defined in VASP were used as the collective variables (CVs). To reduce sampling errors, a fine set of Gaussian hill parameters were used: height 0.0025 eV and width 0.02 CV unit. Gaussian hills were added to the underlying potential energy surface every 20 fs. Metadynamics simulations were terminated after CVs crossed from the reaction basin into the target product basin following a previously reported protocol.[26] The free energy barrier was computed by summing up the amounts of bias potentials accumulated in the reactant basin.

Results and Discussion

Thermal Analysis: Oxidative and thermal degradation of the 45% PEI/ γ-Al_2O_3 sorbent

A model PEI/Al_2O_3 sorbent with PEI loading of 45 wt.% which about 98% pore fill (0.028 cm^3/g) was used for the thermal analysis study. The physical characteristics of the sorbent are determined using N_2 physisorption. TGA-DSC was used to follow the weight loss and heat flow of 28 - 35 mg of the 45 wt.% PEI/ γ-Al_2O_3 sorbent as a function of time. The sorbent was exposed to CO_2-free air (21% O_2) for 3, 7, 10, and 14 days and to 99+% N_2 for 3, 7, and 14

days continuously at 70 °C for oxidative and thermal degradation experiments respectively. The weight loss recorded at 70 °C was assumed to be a result of PEI deactivation. This assumption is supported by the thermogravimetric combustion measurement which shows organic content loss until after 160 °C. **Figure S1** shows the thermogravimetric combustion measurement of the model sorbent (45 wt.% PEI/γ-Al_2O_3). The CO_2 adsorption capacities of the fresh and oxidized samples were determined using 400 ppm CO_2 balance He stream. Sorbent deactivation is defined as the percent loss in CO_2 adsorption capacity (mmol CO_2/g sorbent) from a fresh sorbent after an exposure to a specified gas mixture and deactivation period at 70 °C. The CO_2 adsorption capacity of a fresh sorbent was 1.34 mmol CO_2/g sorbent.

As the results in **Figure 1** show, oxidative and thermal degradation appeared to have similar impact on the loss of adsorption capacity until day 7 (4% vs 3% loss in capacity, respectively). We assign this region of the degradation as "temperature dominant," as most of the impact can be attributed to thermal effects. After day 7, there was more significant sorbent deactivation under oxidative degradation conditions compared to the thermal only conditions. This region is assigned as the "oxidative degradation" dominant region.

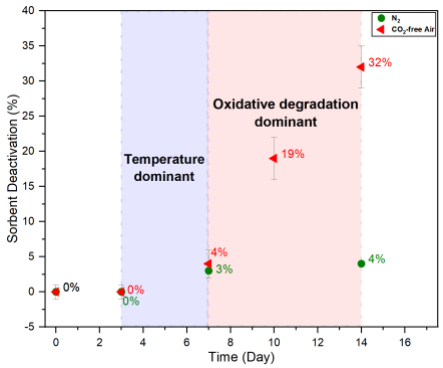

Figure 1. Oxidative and thermal degradation of the 45% PEI/ γ-Al_2O_3 sorbent at 70 °C

Building on these results as a baseline, we then investigated the presence of CO_2 and H_2O together and separately. As shown in **Figure 2**, after 3 and 7 days of continuous exposure to 0.04% CO_2-N_2 flow, the loss in CO_2 adsorption capacity was minimal (3% and 2%, respectively; purple diamonds), indicating limited deactivation. On the contrary, under 0.04% CO_2-air, notable loss in CO_2 adsorption capacity was observed, even in the early stages of deactivation (17% loss after 3 h, blue triangles). Though the deactivation rate is moderate, it eliminates the induction period observed under oxidative and thermal degradation conditions in the absence of CO_2 (**Figure 1**). After 3 h, the deactivation continues to increase, reaching 80% loss after 7 days. Thus, the combination of CO_2 and O_2 leads to more rapid deactivation than with either species alone.

In a humid environment (43% relative humidity (RH); olive triangles), a stream of 0.04% CO_2-air yielded similar deactivation behavior as the dry 0.04% CO_2-air mixture. The initial deactivation rate appeared slightly accelerated under dry conditions and slightly slower at longer times, relative to humid conditions, but these apparent differences are likely within the margin of experimental error. The data in **Figure 2** show that in the absence of CO_2, the differences between dry and humid environments were magnified (dry, red triangles; humid, black squares), with higher deactivation under humid conditions, after 7 days. This difference suggests CO_2 has a bigger impact on oxidative degradation than H_2O under the continuous deactivation conditions explored, with H_2O enhancing degradation in the absence of CO_2. The enhancement of oxidative degradation in the presence of H_2O vapor is consistent with the impact of H_2O in accelerating oxidative degradation reported in our recent work.[17]

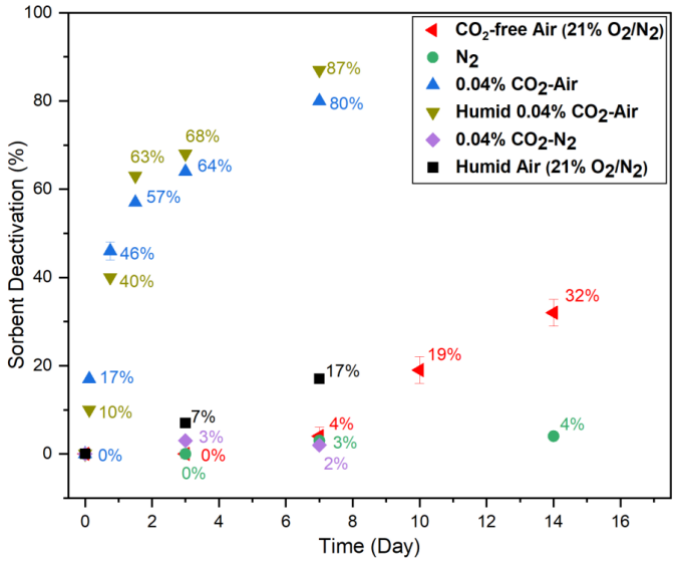

Fig. 2. Deactivation of 45% PEI/ γ-Al_2O_3 sorbent under CO_2-free air (for 3, 7, 10 and 14 days), under N_2 (for 3, 7 and 14 days), under 0.04% CO_2-air (for 3 h, 18 h, 36 h, 72 h, and 7 days, and 0.04% CO_2 balance N_2 environments at 70 °C for 3 and 7 days

The above results (**Figure 2**) show the implications of the co-presence of CO_2 and O_2, as they appear in ambient air, on the stability of amine-based sorbents at an intermediate temperature. As briefly mentioned above, these results differ from what has been reported in the literature over different amine sorbents and under slightly different conditions. Previously, the presence of CO_2 in O_2-containing streams was reported to improve stability of amine-based sorbents based on the fact that amine species react faster with CO_2 compared to O_2, forming carbamate and bicarbonate species that reportedly enhance stability.[10] In the work of Heydari-Gorji et al.,[10] the thermal, oxidative and CO_2-induced deactivation of PEI (branched and linear)-impregnated mesoporous silica (SBA-15) sorbents with platelet particle morphologies and short pore channels was explored. In their specific study pertaining to the co-presence of CO_2 and O_2, a 55 wt.% PEI (branched, M_n ~600)-SBA-15 sorbent was deactivated continuously under pre-humidified $CO_2/O_2/N_2$ streams at different concentrations (1%-20%/10.5%-17%/balance N_2) and temperatures ranging from 50 - 120 °C for 30 h. The lowest CO_2 concentration explored was a 1%/17%/82% ($CO_2/O_2/N_2$) gas mixture. The study reported no significant deactivation below 100 °C for all $CO_2/O_2/N_2$ mixtures. At 100 °C, 70% CO_2 uptake loss was obtained for the 1%/17%/82% ($CO_2/O_2/N_2$) gas mixture after 30 h and the uptake loss decreased significantly as the CO_2 concentration increased to 20% (2.6% loss).[10] In contrast, in the current study, the 45 wt.% PEI/Al_2O_3 sorbent deactivation treatments at 70 °C in both dry and humid 0.04% CO_2-air mixtures yielded noticeable losses in CO_2 adsorption capacity even after 3 h of deactivation (loss of 17% for dry and 10% for humid). Previously, the presence of H_2O was reported to have a positive effect during the oxidative degradation, retarding oxidation;[10] however, as seen in **Figure 2** and as reported in our recent work, the outcome in our system is reversed.[17] When rationalizing these differing results, it is important to note the key differences between the two studies, which include the deactivation temperature (50 – 120 °C for Heydari-Gorji and 70 °C for this study), CO_2 concentration (1-20% for Heydari-Gorji and 0.04% for this study), CO_2 uptake temperature (75 °C for Heydari-Gorji and 30 °C for this study), and support type (lab-synthesized ordered mesoporous silica vs. disordered, commercial mesoporous alumina). Further discussion comparing and contrasting our results to the literature will be presented after additional analysis in the forthcoming sections.

Spectroscopic Analysis

To investigate the accelerated sorbent deactivation in the co-presence of CO_2 and O_2, *in situ* HATR-IR spectroscopy experiments were performed using a branched PEI sample with a molecular weight (MW) of ~800 g/mol as a model sorbent. Experiments were conducted using different gas/vapor compositions, including dry CO_2-free air, 0.04% CO_2-air (21% O_2 balance N_2), and 0.04% CO_2-N_2 at 70 °C for 7 days (**Figures 3 and S2**). Complementing the TGA studies above, these experiments allow the elucidation of molecular level changes due to PEI deactivation under the above conditions and investigation of possible changes in the PEI structure. Before every experiment, the sorbent

was pretreated at 100 °C for 1 hour under N_2 to remove adsorbed species (such as H_2O and CO_2) acquired during sample storage or preparation steps. After pretreatment, the temperature was reduced to 70 °C, and the samples were deactivated under a continuous flow of dry gas for 7 days. Spectra were collected every 30 minutes. **Figures 3** and S2 show the absorption spectra of PEI over 7 days at 70 °C under the three experimental conditions.

The main characteristics of branched PEI in the infrared spectra are two N-H stretching bands of primary amines (3400 – 3300 cm^{-1} and 3330-3250 cm^{-1}), one of secondary amines (3350-3310 cm^{-1}), C-H stretching bands (2950 – 2720 cm^{-1}), an N-H bending band ~ 1590 cm^{-1}, and a C-H bending band ~ 1454 cm^{-1}.[27]

In the early phase of the deactivation of PEI under 0.04% CO_2-N_2 at 70 °C, adsorbed CO_2 dominated the difference spectra since the thermal deactivation of PEI should contribute only minimally to the spectral changes under these conditions (see **Figure 1**). **Figures 3a and 3b** show bands of species such as COO^-(~1430 cm^{-1}), N-COO (~1330 cm^{-1}) and NH_2^+ at 1630 cm^{-1}, which indicate the formation of ammonium carbamate ion pairs in the early stages of the experiment and their growth in intensity with time.[28-41] In CO_2 capture studies using amines like PEI, the dominant species that form due to the interaction of CO_2 with primary and secondary amines under dry conditions are carbamate species.[28, 30, 41-44]

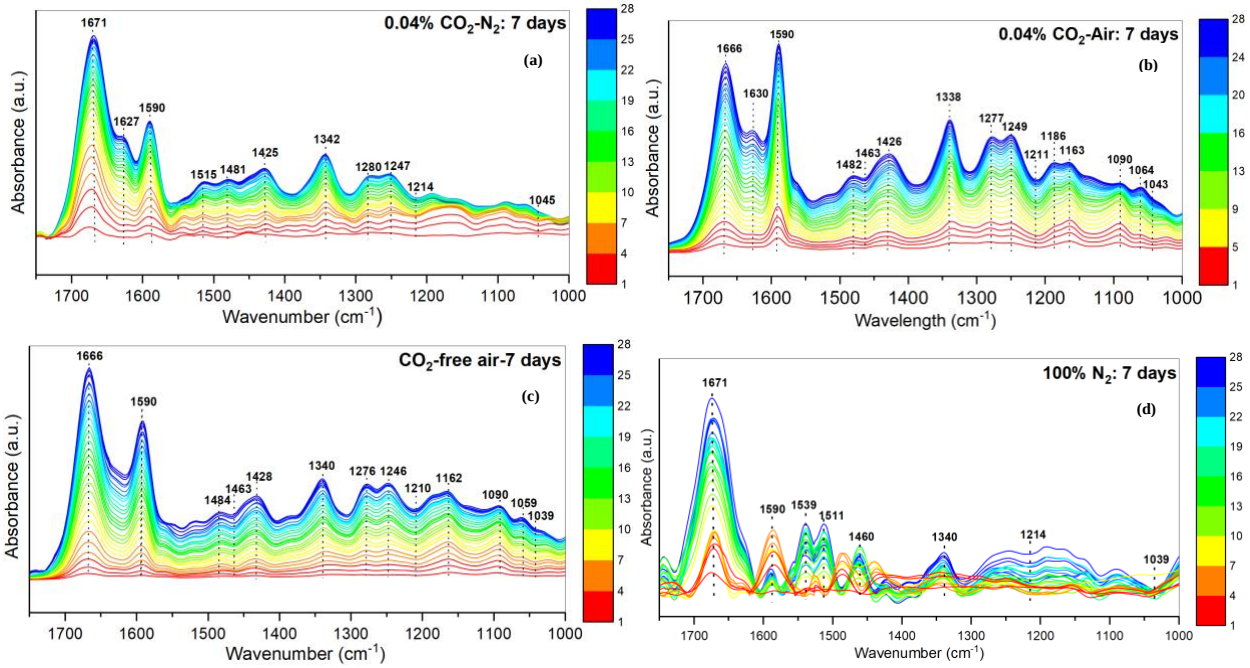

Figure 3. IR spectra (1800 – 1000 cm^{-1}) of PEI deactivation under (a) 0.04% CO_2-N_2, (b) 0.04% CO_2-air (21% O_2-N_2), (c) CO_2-free air, and (d) 100% N_2 for 7 days (168 hours with 6 hours gap between each spectra shown)) at 70 °C. (Full spectra (3500 – 1000 cm^{-1}) in **Figure S2.**

Figure 3(a-d) also shows bands in the region of 1666 - 1671 cm^{-1} that increase in intensity as the treatment time increases. This band has been discussed in the literature as characteristic of amine-related oxidation products as a result of exposure to O_2 and has been assigned to vibrations of C=N (imines) and/or C=O (carbonyl) groups.[27, 36, 39, 45, 46] A recent study from our group on the oxidative degradation of PEI/γ-Al_2O_3 sorbent at high temperatures illustrated the individual contributions of the imine and carbonyl species to the band in the region around 1666 cm^{-1} for the first time.[17] The study links C-N bond cleavage events to the formation of carbonyl and imine species, new primary amine species, and other low molecular weight amine products.[17] To briefly discuss the proposed mechanism(s), in dry conditions, degradation begins with the formation of radical species (α- or β-amino alkyl radicals) due to thermal stress, which leads to chain relaxation and breakage,[17] or due to metal impurities within the sorbent that catalyze free radical formation.[17, 47] In the presence of O_2, the radical species react quickly with O_2 forming peroxyl radical species

(α- or β-amino peroxyl radicals). The peroxyl radicals extract hydrogen from the PEI chain, forming hydroperoxide species (ROOH), which decompose to form carbonyl species in the PEI chain.[17] The formation of the carbonyl species requires cleavage of the C-N bond and depending on the location of the C-N bond (terminal primary amine, terminal secondary amine, or secondary amine along the PEI chain), volatile organic products (e.g., ammonia and 2-aminoacetaldehyde) and new primary amine species can form.[17, 48]

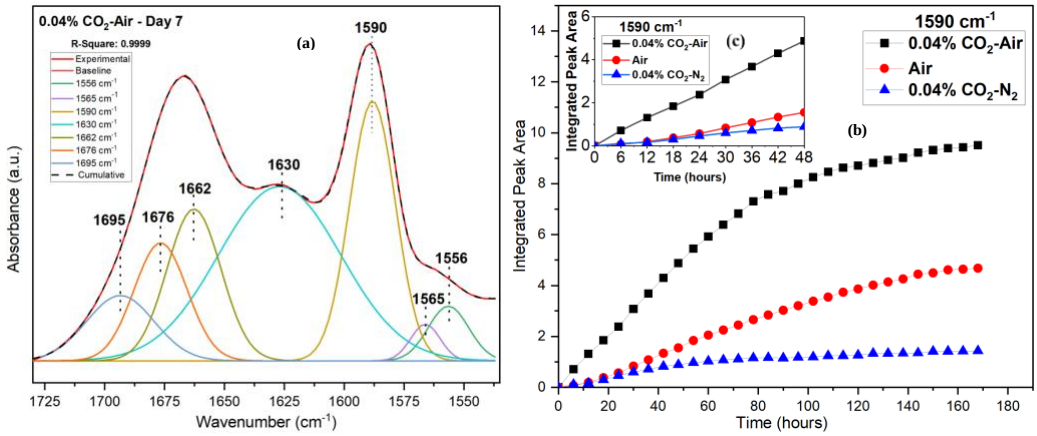

Figure 4. (a) Deconvoluted spectra of 0.04% CO_2-air at the 168th hour (end of day 7) from 1730 cm^{-1} – 1520 cm^{-1} (b) Integrated peak area of 1590 cm^{-1} (N-H bending band) for the three conditions studied for 7 days (168 hours) (c) for 48 hours deactivation

In this study, a similar deconvolution analysis was performed in the region between 1750 cm^{-1} and 1500 cm^{-1} to distinguish contributions of the imine and carbonyl species to the 1666 cm^{-1} band under 0.04% CO_2-air and 0.04% CO_2-N_2 conditions. **Figure 4a** shows the results of the deconvolution analysis of the 0.04% CO_2-air condition. Three peaks (1695 cm^{-1}, 1676 cm^{-1} and 1662 cm^{-1}) contributed to the 1666 cm^{-1} band. The contribution at 1662 cm^{-1} can be attributed to carbonyl species (C=O) on the PEI chain while the one at 1676 cm^{-1} can be assigned to imine species (C=N).[17, 27] Another interesting outcome of the deconvolution of the peaks in **Figure 4a** are the bands at 1695 cm^{-1}, 1565 cm^{-1}, and 1556 cm^{-1}. These bands can be attributed to the formation of urea linkages, reported in the literature as U-2 or U-4.[11, 49] Similar to the intensity shown in **Figure 4a**, these bands were also reported to have relatively weak peaks.[10, 11, 49, 50] The weak intensity is expected, as the likelihood of the formation of urea species at an intermediate temperature of 70 °C and CO_2 concentration of 0.04% is low.[49] The band at 1630 cm^{-1}, which represents NH_2^+ deformations, appears only during PEI deactivation under 0.04% CO_2-air (and under 0.04% CO_2-N_2 as mentioned above) as a result of the formation of alkyl ammonium carbamate ion pairs.[38] The 1630 cm^{-1} band might also be ascribed to the bending vibration of H_2O vapor,[51] however, considering the higher concentration of CO_2 in the system compared to H_2O, it is most likely a contribution from alkyl ammonium carbamate ion pairs.

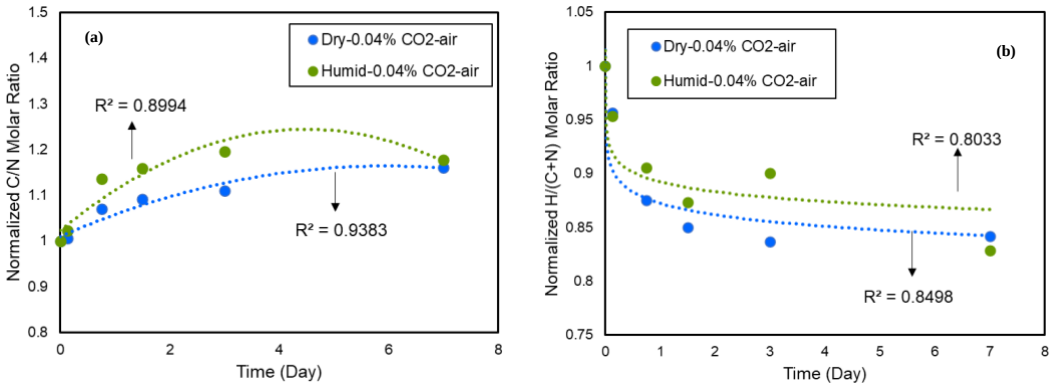

Figure 5. (a) C/N (b) H/(C+N) molar ratio of deactivated 45 wt.% PEI/γ-Al_2O_3 sorbent as a function of time under dry 0.04% CO_2-air and humid 0.04% CO_2-air

Figure 4a also shows the band at 1590 cm^{-1}, which represents an N-H bending (N-H deformation) mode,[17, 27, 40] had no additional contributing peaks. N-H bending/deformation vibration bands appear in the region between 1650 – 1580 cm^{-1} for primary and secondary amines species.[27] Furthermore, in liquid amines, the N-H bending band gives rise to a shoulder/overtone band near the N-H stretching regions that can be seen from the band around 3135 cm^{-1} in **Figure S2(a-d)**.[27] As briefly discussed above, the increased intensity of the 1590 cm^{-1} band has been reported in our recent work as an indication of the formation of new primary amine species as a result of C-N bond cleavage near secondary amine sites.[17] Similarly, **Figure 3(a-c)** showed an increase in the intensity of the bands around 1590 cm^{-1} with time for 0.04% CO_2-N_2, 0.04% CO_2-air, and CO_2-free air. The integrated area of the peak at 1590 cm^{-1} for the sample treated in 0.04% CO_2-air was much larger than that for the samples under CO_2-free air and 0.04% CO_2-N_2 (**Figure 4b**). This result suggests that the formation of new primary and secondary amine species and C-N bond cleavage reactions occur more frequently in the co-presence of CO_2 and O_2, which agrees well with the thermal analysis results shown in **Figure 2,** where deactivation of the PEI/γ-Al_2O_3 sorbent is more significant under a 0.04% CO_2-air environment compared to a CO_2-free air and 0.04% CO_2-N_2 environments. The disproportional loss of hydrogen and nitrogen species with respect to carbon species is shown by C/N and H/(C+N) molar ratios in **Figure 5a and 5b** during the deactivation of the sorbent under both dry and humid 0.04% CO_2-air conditions. The higher loss of N and H content compared to C content is an additional sign of the C-N bond cleavage indicated by the spectra in **Figure 3b**. **Figure S3** also shows the loss of hydrogen and nitrogen species and an increase of carbon species under both dry and humid conditions.

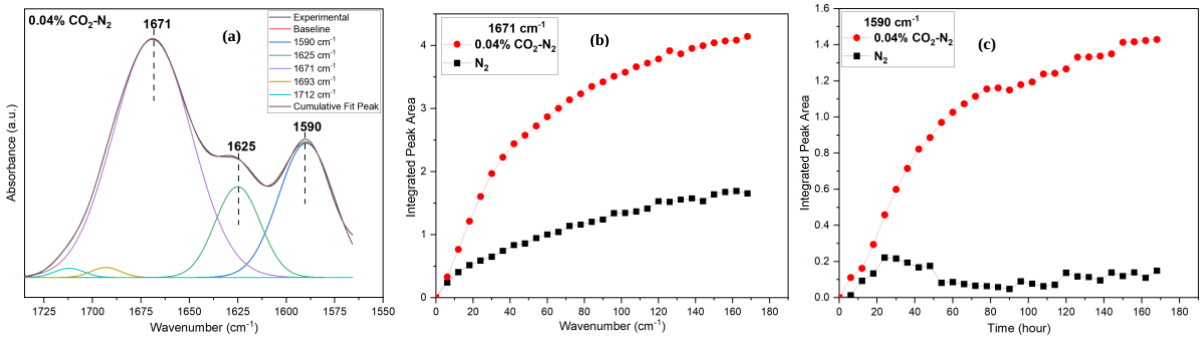

Figure 6. (a) Deconvoluted spectra of 0.04% CO_2-N_2 at the 168th hour (end of day 7) from 1730 cm^{-1} – 1520 cm^{-1}, Integrated peak area for 0.04% CO_2-N_2 and pure N_2 for 7 days (168 hours) (b) 1671 cm^{-1} (C=N stretching band) (c) 1590 cm^{-1} (N-H bending band)

Figure 3(a-d) also shows an increase in the 1666 cm^{-1} band intensity for CO_2-free air and 0.04% CO_2-air and in the 1671 cm^{-1} band intensity for 0.04% CO_2-N_2 and N_2. The increase in the 1666 cm^{-1} band can be attributed to the formation of carbonyl and imine species, as shown from the deconvolution results in **Figure 4a,** and from evidence for C-N bond cleavage reaction as also indicated by the negative bands at 1211 cm^{-1} and 1050 cm^{-1} for 0.04% CO_2-air and at 1210 cm^{-1} and 1039 cm^{-1} for CO_2-free air. Similarly, the 1671 cm^{-1} band can be attributed to the formation of imine species due to the absence of O_2 in the deactivating mixture (**Figure 3a and 3d**). To confirm the contribution of imine species to the 1671 cm^{-1} band, we performed deconvolution of peaks in the region between 1750 cm^{-1} and 1500 cm^{-1} for sample treated in 0.04% CO_2-N_2. As shown in **Figure 6a,** only one main peak contributed to the 1671 cm^{-1} band and that is the imine species. Comparing the integrated peak areas of the 1671 cm^{-1} band for the samples treated in 0.04% CO_2-N_2 and N_2 highlights the significant difference in the integrated peak area between the two deactivating environments, where the peak area for the sample treated in 0.04% CO_2-N_2 was higher (**Figure 6b**). While this result suggested more deactivation under 0.04% CO_2-N_2 compared to N_2 alone due to more frequent C-N bond cleavage, the thermal analysis results for the deactivation of the PEI/γ-Al_2O_3 sorbent in a 0.04% CO_2-N_2 and N_2 environment at 70 °C showed similar deactivation (**Figure 2**). This may be due to differences in the C-N bond cleavage sites between the two conditions/environments, where in a CO_2-N_2 environment C-N cleavage forms amines that participate in adsorbing CO_2, maintaining CO_2 capture performance (**Figure 2**), or that the radical species that form are stabilized by reacting with each other, terminating the deactivation, and maintaining sorbent stability. The change

in the 1590 cm^{-1} band shown in **Figure 6c** supports the former hypothesis, as it indicates new primary amine formation under a 0.04% CO_2-N_2 environment and a relatively consistent total number of primary amine species under the N_2 environment.

C-N bond cleavage leading to the formation of new primary amine species (as well as other products mentioned above) has been reported as paths of oxidative and thermal degradation at high temperatures in solid amine sorbents.[16, 17, 48] As such, these results suggest the possible occurrence of oxidative and thermal degradation under CO_2-free air and 0.04% CO_2-air conditions and thermal degradation under 0.04% CO_2-N_2 and N_2 conditions. However, the accelerated PEI/γ-Al_2O_3 sorbent deactivation and new primary amine species formation under 0.04% CO_2-air, as shown in **Figure 2 and 4b,** along with the significant differences in the 1671 cm^{-1} and 1590 cm^{-1} bands between the 0.04% CO_2-N_2 and N_2 cases, as shown in **Figure 6a,** indicate the presence of additional reaction mechanism(s) occurring in the presence of CO_2.

Metadynamics simulations

A previous modeling study by Li et al. used triethylenetetramine (TETA) as a molecular proxy for PEI and accessed the kinetic feasibility of C-N bond cleavage in the presence of radicals but without CO_2 using enhanced sampling, i.e. metadynamics, simulations.[16] To this end, we performed first-principles metadynamics simulations using CO_2-bound TETA as a molecular proxy to analogously evaluate the kinetics of C-N bond cleavage of PEI under CO_2-air conditions.

To model the interactions between CO_2 and amines, we constructed bimolecular structural models consisting of one TETA with CO_2 adsorbed to a primary amine site as carbamic acid. CO_2 adsorbed as an ammonium carbamate ion pair will behave similarly due to dynamic equilibrium between a hydrogen bonded carbamic acid-amine pairs and the ammonium carbamate. The adsorbed CO_2 further interacts with either a primary or secondary amine on another TETA with a preformed alkyl radical, presumably resulting from radical propagation under oxidative conditions. The AIMD-equilibrated structures are presented in **Figure 7** and were prepared for metadynamics simulations with a temperature set at 70°C to replicate the experimental conditions. The metadynamics approach adds periodic biasing potentials to the original potential surfaces along predefined collective variables (CVs), which discourage the system from revisiting points in the configurational space, resulting in the acceleration of energy barrier crossing for the sampled reactions.[52] To determine the kinetics of C–N bond cleavage, two CVs were defined: C–N coordination number (CN_{C-N}) and N-H coordination number (CN_{N-H}) of amines interacting with the carbamic acid in proximity.

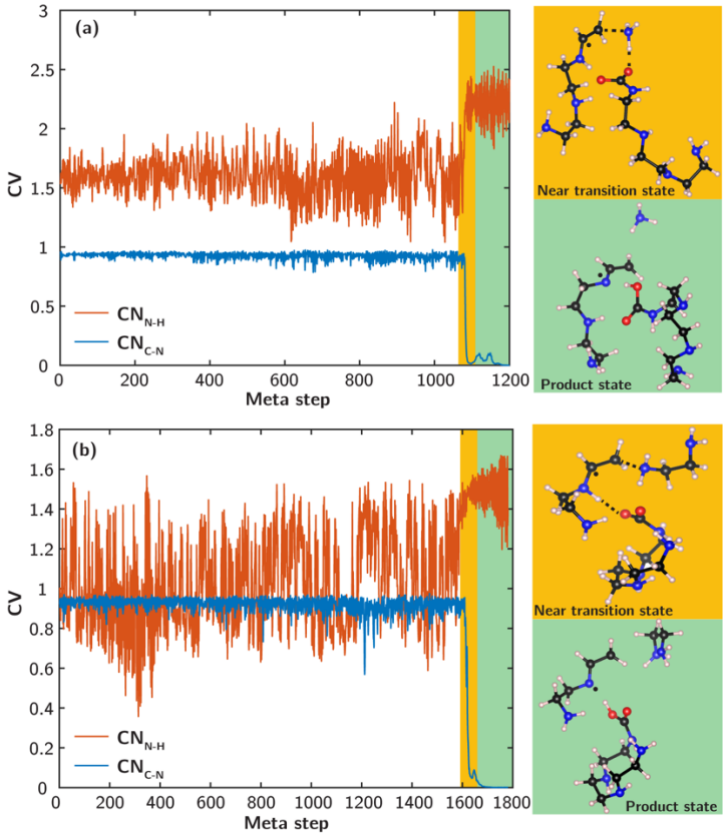

Figure 7. Time evolution of CVs along the trajectories of metadynamics simulations of CO_2-catalyzed C–N bond cleavage near (a) primary amine and (b) secondary amine. Structural snapshots near transition states and product states are shown. Atom color code: C–black, N–blue, O–red, H–pink.

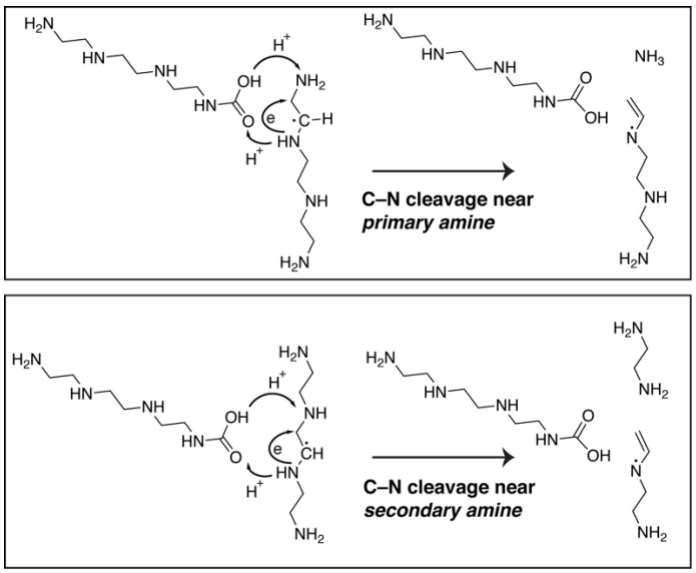

Scheme 1. Reaction pathways of C–N bond cleavage near primary and secondary amines in the presence of CO_2

Figure 7 displays the evolution of CVs during metadynamics simulations for C–N bond cleavage near primary and secondary amines. The successful cleavage of C–N bonds is observed in both cases, as evidenced by sharp decreases in CN_{C-N} from approximately 1 to 0. Additionally, simultaneous increases in CN_{N-H} and structural snapshots near

transition states demonstrate that for both primary and secondary amines, H transfer occurs from a neighboring amine group to the affected amine, resulting in the formation of NH_3 and ethylene diamine, respectively. **Scheme 1** illustrates that carbamic acids function as effective H-shuttles, facilitating the proton and electron transfer necessary to cleave the C-N bonds. The products consist of fragments of TETA and a regenerated TETA with a carbamic acid tail. The formation of a new primary amine in the case of C–N bond cleavage near secondary amine is consistent with observations from spectroscopic experiments. Significantly, the sum of the biasing potentials indicates that in the presence of CO_2, both reactions of C–N bond cleavage have free energy barriers of ~ 20 kJ mol^{-1}, which is considerably lower compared to that in the absence of CO_2 (~ 90 kJ mol^{-1}).[16] This manifests the strong catalyzing effect of CO_2 on the C–N bond cleavage kinetics through acid-base interactions, consistent with the accelerated PEI/γ-Al_2O_3 sorbent deactivation under 0.04% CO_2-air conditions.

Based on the spectroscopic, thermal, and elemental analysis and metadynamics simulations performed in this study and the accumulated knowledge in the aminopolymer degradation literature, we rationalize the accelerated deactivation in the co-presence of CO_2 and O_2. **Figure 4c** shows that in the first 24 hours of deactivation, the rate of formation of new primary amines is similar for 0.04% CO_2-N_2 and CO_2-free air, but after 24 hours the formation rate under CO_2-free air is much higher (**Figure 4b**). However, the thermal analysis data in **Figure 2** showed that the deactivation under both conditions was similar, even after 7 days. The similarity in deactivation between the two conditions suggests that under a CO_2-free environment, the C-N cleavage process occurs at a slower rate (compared to 0.04% CO_2-N_2). Based on the oxidative degradation pathway proposed in our recent work[17] and the basic autoxidation mechanism,[51] the slower rate of C-N cleavage is likely due to the substantial energetic barrier for the decomposition of hydroperoxide species to hydroxyl and alkoxyl radical species in the oxidative degradation process.[51] The deactivation temperature studied here (70 °C) is most likely not sufficiently high to allow the decomposition process to occur rapidly. In the co-presence of CO_2 and O_2 (0.04% CO_2-air), CO_2 reacts with amine sites forming carbamic acids that can further react with primary or secondary amines in the surrounding region via acid-base interactions. Some of these species become captured CO_2 in the form of alkyl ammonium carbamates, while some facilitate H-transfer and C-N bond cleavage forming ammonia, primary amine, or secondary amine species, depending on the site of CO_2 adsorption, as supported by metadynamics simulations. This acid catalyzed process requires the presence of alkyl radicals on the PEI chain where C-N cleavage occurs. Oxygen, which is present in much higher concentration than CO_2, can then participate in the formation of peroxyl radicals that abstract hydrogen atoms, leading to more alkyl radical species in what appears to be a carbamic acid catalyzed decomposition reaction. As a result, the carbamic acid catalyzed deactivation is proposed to provide an alternative pathway for the C-N bond cleavage that bypasses the hydroperoxide decomposition step and subsequently accelerates the deactivation and formation of the various species discussed above.

Adsorption-Desorption Cycles

Cyclic adsorption-desorption experiments were performed to develop relationships with the continuous deactivation study under dry and humid 0.04% CO_2/air (21% O_2 balance N_2) conditions at 70 °C and to observe sorbent deactivation under close-to-realistic DAC process conditions. A typical cyclic process involves adsorption of CO_2 from the atmosphere, consuming most of the process time, followed by desorption of CO_2 captured from the atmosphere, and finally cooling of the sorbent to the adsorption temperature. During these adsorption-desorption processes, sorbent materials are exposed to conditions and environments that cause deactivation over an extended period of operation. In practice, on occasions where process upsets occur due to operational malfunctions or for other reasons, additional deactivation factors are introduced, such as the co-presence of high temperatures and high oxygen concentrations.

In these cyclic studies, the 45 wt.% PEI/γ-Al_2O_3 sorbent was exposed to dry or humid (43% RH or 12 mmol H_2O/mol air absolute humidity) 0.04% CO_2-air for 2 hours, which represents roughly two thirds of the laboratory process/cycle time. The captured CO_2 is desorbed at 100 °C for 30 minutes under dry N_2 or humid N_2 (1.3% RH (absolute humidity of 12 mmol/mol)) to mimic the vacuum assisted desorption during a temperature-vacuum swing desorption process. After 30 minutes of desorption, the temperature is ramped down to 70 °C under N_2 (dry or humid). Following that, the sorbent is cooled to the adsorption temperature of 30 °C under dry or humid 0.04% CO_2/air (21% O_2 balance N_2).

This cooling step is typically performed in an inert environment such as N_2 in prior literature studies of amine sorbent stability; the conditions here more closely mimic those that might be encountered in practical operation. The cooling process takes about 30 minutes on average in the laboratory, but would be more rapid in realistic, low pressure drop gas-solid contactors. Cooling the sorbent under CO_2 containing air (atmospheric concentration air) removes the use of inert gases in this step, which is common in the laboratory, and it allows for CO_2 to be captured during the cooling process. In addition, cooling using atmospheric concentration air eliminates the use of inert gas, reducing energy and process cost. **Figure 8** shows the adsorption-desorption cycle used in this study.

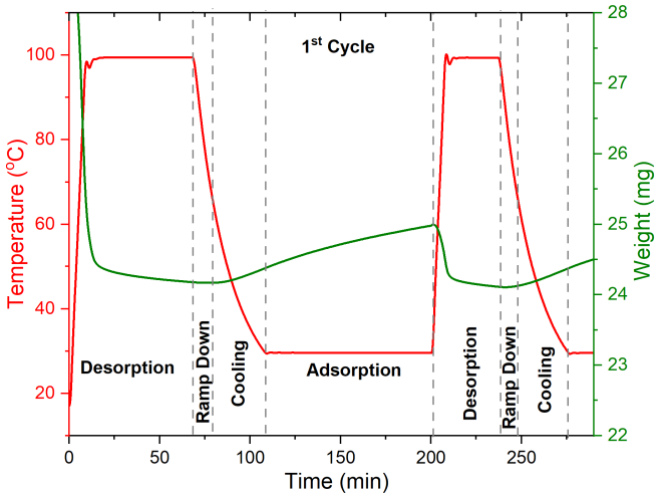

Figure 8. Adsorption – desorption cycle deployed in TGA cycling.

During the adsorption and cooling process, the sorbent interacts with O_2 and CO_2 at low and intermediate temperatures after desorption in flowing N_2 (simulating vacuum) at higher temperatures. In this cyclic process, the most important time when oxidative deactivation would be a concern is during the cooling process where the sorbent is exposed to intermediate temperatures under the co-presence of CO_2 and O_2 leading up to the next adsorption step. The results in **Figures 9a and 9b** show that 30 adsorption-desorption cycles result in a CO_2 uptake loss of 23% under dry and 48% humid conditions, as well as a gradual loss in sorbent mass (~6% for dry and ~4% for humid). Consistent with the continuous deactivation study in **Figure 2,** the co-presence of CO_2 and O_2 results in noticeable deactivation under cyclic conditions, and the use of consecutive cycles seeks to ascertain if numerous short exposures begin to approach the deactivation of extended exposure times.

Another interesting finding from this study is that during continuous deactivation, the presence of H_2O only slightly affected sorbent deactivation in the co-presence of CO_2 and O_2 as shown in **Figure 2**. On the contrary, under cyclic conditions, the presence of H_2O shows considerable deactivation after 30 cycles compared to the dry cyclic condition (about 2X higher). This might be due to H_2O gaining more access to the PEI domain and radical species in the absence of CO_2 (desorption and ramp down step) which can lead to accelerated deactivation.[17] Notably, this result is consistent with our recent finding on the effect of humidity in accelerating sorbent deactivation which shows 2X faster deactivation under in the presence of H_2O conditions.[17] It is important to note that the cyclic CO_2 uptake under humid conditions was determined by performing the same cyclic experiment under humid N_2 for 15 cycles and then subtracting the H_2O vapor uptake from that measured in the 0.04% CO_2-air humid cyclic experiment. During the humid N_2 cyclic experiment, the H_2O adsorbed per cycle was around 2.2 mg (shown in **Figure S4**). In the 0.04% CO_2-air humid cyclic experiment, this amount will most likely be less than 2.2 mg due to the competitive interaction between CO_2 and H_2O vapor with amine sites during the adsorption step. As such, the CO_2 uptake reported in **Figure 9b** for the humid cyclic condition likely slightly underestimates the actual capacity.

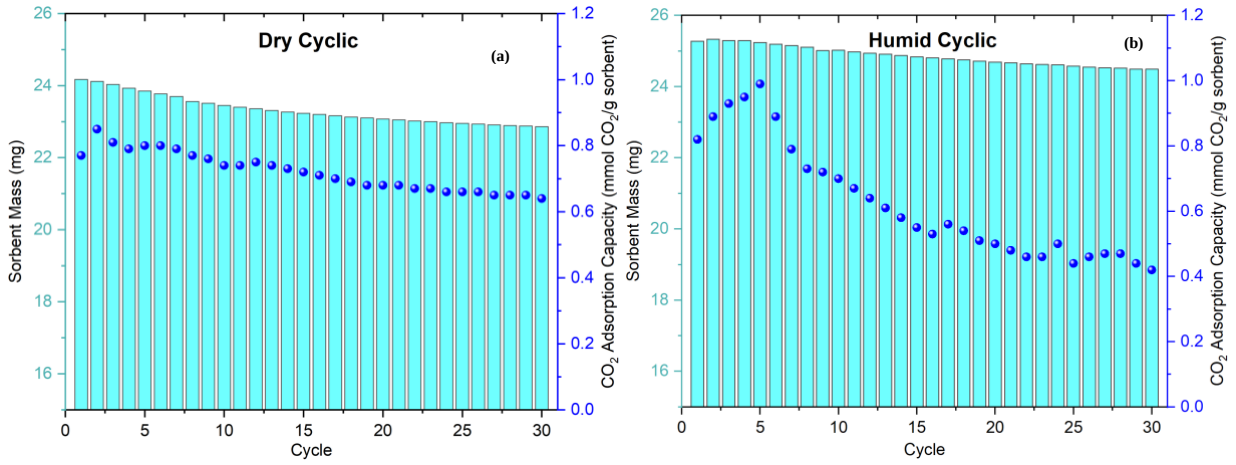

Figure 9. Sorbent mass and CO_2 adsorption capacity change after 30 cycles under dry (a) humid (b) 0.04% CO_2-air.

The total time the sample was exposed to elevated temperature, during the desorption step at 100 °C and the cooling step from 100 to 70 °C, sums up to approximately 17 hours across the 30 cycles. During these steps, the sample is only exposed to inert atmosphere, and so thermal degradation due to loss of sorbent mass is the dominant loss mechanism, 6% and 4% for the dry and humid cyclic conditions respectively.

The total time the sample was exposed to oxygen, during the cooling step from 70 to 30 °C and the following 2-hour adsorption step at 30 °C, sums up to approximately 3 days across the 30 cycles. Therefore, it is reasonable to compare the loss in capacity across the cyclic experiment with the 3-day continuous deactivation experiment. Under both conditions, the loss in capacity under the cyclic conditions is lower (dry: 29% vs 64%, humid: 52% vs 68%). This difference in capacity loss shows that continuous exposure exaggerates deactivation. However, continuous deactivation studies can help estimate the lifetime of a sorbent over an extended period of operation if suitable correlations can be developed for real operation. As such, below we will use the deactivation mechanism(s) presented in **Scheme 1** to rationalize the differences in capacity loss between the continuous and cyclic conditions.

One of the primary reaction intermediates in the deactivation of the sorbent, the peroxyl radicals, forms by the reaction of alkyl radicals with molecular oxygen. Peroxyl radicals form at similar rates at any temperature once alkyl radicals form and the sorbent is exposed to an O_2 containing stream.[51, 53] However the subsequent step of the reaction, the formation of hydroperoxide species, requires the abstraction of a hydrogen atom from a C-H bond, and this reaction is temperature dependent. At higher temperatures, more energy is available to overcome the activation energy required for the hydrogen abstraction.[51, 53] Similarly, the rate of decomposition of hydroperoxide species to alkoxyl and hydroxyl radical species increases with temperature.[51, 53] As such, during the cooling (from 70 °C to 30 °C) and adsorption step (at 30 °C) of the cyclic process, it is expected to have a lower concentration of hydroperoxide species and the decomposition of hydroperoxide species to occur at a slower rate compared to continuous deactivation cases at 70 °C. It is also important to note that during the cyclic process, the limited co-existence of O_2 and heat compared to the continuous deactivation likely plays a role in maintaining sorbent stability. Correspondingly, during the cooling and adsorption periods of the cyclic process, recombination reactions of radical species may occur, causing the sorbent to "recover" some stability. These reasons combined lead to delayed deactivation in the cyclic processes. Furthermore, in industrial-scale adsorption-desorption units, the adsorption, desorption, and cooling time are much shorter than the conditions used in this cyclic study, leading to even slower sorbent deactivation. In the **Supporting Information** we provide various simple mathematical fits based on the cyclic deactivation data to estimate sorbent lifetime. However, high fidelity predictions require a much larger data set than is available here.

Like the continuous deactivation studies, we compare and contrast our results from the cyclic experiments with the literature. To the best of our knowledge, there have not been any adsorption-desorption cyclic studies on the impact of the co-presence of CO_2 and O_2 in amine sorbent degradation under dry and humid conditions. The closest relevant example is the study by Heydari-Gorji et al., which performed cyclic studies under humid and dry pure CO_2

(adsorption at 75 °C and desorption at 105 and 120 °C under N_2 for 30 mins each) and humid 15% CO_2/N_2 (adsorption at 50 °C and desorption at 85 °C under humid N_2 for 30 mins each) for 66 cycles. Their results showed a significantly higher loss in CO_2 uptake under the dry conditions compared to the humid conditions studied (dry: 40% and 52% loss, humid: 2% and 3.5% loss, at 105 and 120 °C desorption conditions, respectively).[10] Similar to the pure humid CO_2 conditions, the sample treated in humid 15% CO_2/N_2 also showed relatively little loss after 66 cycles.[10] The authors attributed the significant loss under dry conditions to urea formation due to exposure to high CO_2 concentrations. In the presence of humidity, however, urea formation is suppressed, and sorbent stability is maintained.[10]

To rationalize the discrepancy in the continuous deactivation behavior of the two studies, we consider the major differences between the two studies, including support type, CO_2 uptake temperature, and CO_2 concentration. First, we note that γ-Al_2O_3, the mesoporous oxide support used in this study, is often produced by extracting alumina from metakaolin, a dehydroxylated form of the clay mineral kaolinite.[54] As a result, γ-Al_2O_3 often has trace metal impurities in higher concentration than laboratory synthesized silica supports, as used by Heydari-Gorji et al.[10] Mesoporous silica SBA-15, often synthesized in the laboratory from Pluronic P-123 and tetraethyl orthosilicate (TEOS), has notably lower transition metal impurities due to the use of TEOS in the synthesis.[55] Metal impurities are one of the key contributing factors in initiating alkyl radical species formation and accelerating sorbent deactivation.[47] A recent study from our group reported higher metal impurities (mainly Fe and Ni) in γ-Al_2O_3 (similar to the γ-Al_2O_3 used in this study) compared to SBA-15.[17] The presence of such transition metals in higher concentration can lead to O_2 activation, accelerating oxidation reactions, thereby catalyzing the sorbent deactivation process. As such, the higher concentration of metal impurities in γ-Al_2O_3 compared to SBA-15 is one likely reason for the differences observed in the loss in CO_2 uptake between the two studies.

Additional factors that also may contribute to the differences in stability are the conditions used for the CO_2 uptake measurement during and after deactivation experiments (specifically CO_2 concentration and CO_2 uptake temperature). In the study by Heydari-Gorji et al.,[10] long-term deactivation experiments were performed under different $CO_2/O_2/N_2$ concentrations (1%-20%/10.5%-17%/balance N_2) and temperatures ranging from 50 - 120 °C for 30 h, whereas in this work deactivation experiments were performed under 0.04% CO_2-air, 0.04% CO_2-N_2 and CO_2-free air at 70 °C. Our first-principles modeling indicates that adsorbed CO_2 significantly decreases the free energy barrier of C-N bond cleavage, likely altering the oxidation rate-determining step from C-N bond cleavage (either through direct cleavage or alkyl hydroperoxide decomposition[48]) to radical propagation that generates the necessary on-site alkyl radicals before cleaving C–N bonds. In the CO_2 concentrations explored in the Heydari-Gorji et al. study, the interaction of amines and CO_2 occurs quickly. This rapid interaction between CO_2 and amine sites due to the high concentration of CO_2 interlocks amine chains, slowing down radical propagation, likely preventing carbamic acid catalyzed C-N bond cleavage from occurring and additional CO_2 and O_2 from fully accessing the polymer domains. Consequently, in the work of Heydari-Gorji et al., sorbent stability was more effectively maintained under the deactivation conditions explored. This hypothesis is consistent with studies probing the diffusion of CO_2 through supported PEI as a function of CO_2 concentration and time, where concentrated CO_2 rapidly crosslinks amine chains and limits further CO_2 and O_2 penetration into the bulk of the sorbent,[56] as well as studies that invoke such behavior to rationalize cases where comparable CO_2 uptakes were achieved at both air and flue gas CO_2 concentrations.[57]

Conclusion

The impact of O_2, CO_2, and H_2O on the long-term stability of PEI/Al_2O_3 sorbent is evaluated using TGA, *in situ* HATR-IR spectroscopy, metadynamics calculations, and elemental analysis techniques at an intermediate temperature of 70 °C. The thermal analysis results for oxidative and thermal degradation show a similar impact on the sorbent stability until day 7 where thermal effects are dominant. After day 7, the oxidative degradation condition becomes dominant, showing significant sorbent deactivation compared to the exclusively thermal conditions. In the co-presence of CO_2 and O_2 (0.04% CO_2/ 21% O_2) in both humid and dry streams, sorbent deactivation is further accelerated, eliminating the induction period observed in the early stages of oxidative degradation experiments.

In situ HATR-IR study of PEI deactivation in the presence of CO_2 and O_2 reveals that the presence of CO_2, which leads to surface carbamic acid and ammonium carbamate species, contributes to accelerated oxidative degradation. HATR-IR spectra over 7 days of deactivation show the formation of new primary amine, carbonyl, and imine species which is evidence for C-N and C-H bond cleavage due to oxidative degradation. Based on metadynamics calculations, we hypothesize that carbamic acid species can catalyze the cleavage of C-N bonds on adjacent amine chains that contain a carbon-based radical, leading to loss of some amine binding sites. Interestingly, prior literature by Heydari-Gorji et al.[10] showed that in the presence of higher concentrations of CO_2 and lower concentrations of O_2, H_2O and CO_2 protect amines from oxidative or thermal degradation reactions. Our analysis attributes this differing behavior to two major factors. First, the alumina supports used in this work likely contain larger concentrations of transition metal impurities, which can catalyze oxidative degradation reactions, compared to the silica supports used by Heydari-Gorji et al. in their study that focused primarily on flue gas conditions. Additionally, under DAC conditions, the kinetics of CO_2 uptake are slower than under flue gas conditions. We hypothesize that longer-lived carbamic acid species that form in a dilute CO_2 stream can catalyze the decomposition of adjacent amine chains that contain carbon centered radical species, as supported by metadynamics calculations. In contrast, CO_2 sorption is much more rapid under flue gas conditions, leading to short-lived carbamic acid species and predominant alkyl ammonium carbamate species formation, which crosslinks the amine chains and prevents deep penetration of CO_2 and O_2 species into the polymer domains. We hypothesize that this limits CO_2-induced deactivation under flue gas conditions.

Sorbent stability studies under close-to realistic cyclic DAC conditions (30 adsorption-desorption cycles) show a gradual loss in stability (dry: 29%, humid: 52%) under CO_2-containing air conditions (0.04% CO_2/21% O_2 balance N_2). The loss in capacity during the sorption/desorption cycling is significantly less than the degradation under continuous deactivation conditions, as expected.

The main limitations to this study include (i) the use of a TGA for cycling experiments, which differs in flow characteristics from practical DAC gas/solid contactor mased on monoliths, fibers or laminates, and the (ii) differing cycle times that results from such TGA use, compared to the more practical contactors. Additionally, desorption is done under gas purge in these studies, instead of through use of vacuum and/or steam flow, which are favored in some large-scale process designs. Finally, the work here and elsewhere[17] demonstrates that sorbent degradation is impacted by the nature of the supports used, so further extrapolation is not facile to other systems. Nonetheless, performing studies at these close-to realistic conditions (compared to exiting literature studies) aids close comparison to industrial scale DAC operations and provides means for the expedited development and implementation of sorbent materials with significantly improved stability.

Acknowledgments
This work was initiated with financial support from Global Thermostat. This work was supported by the U.S. Department of Energy (DOE), Office of Science, Basic Energy Sciences, Materials Science and Engineering Division. Work at LLNL was done under the auspices of the U.S. DOE Contract DE-AC52-07NA27344. Computation resources were provided by the LLNL Grand Challenge Program.

Conflicts of Interest
The authors declare the following competing financial interest(s): C.W.J. has a financial interest in Global Thermostat, which seeks to commercialize CO_2 capture from air. This work is not affiliated with Global Thermostat. C.W.J. has a conflict-of-interest management plan in place at Georgia Tech.

References
(1) The IPCC Sixth Assessment Report on Climate Change Impacts. *Popul Dev Rev* **2022**, *48* (2), 629-633. DOI: 10.1111/padr.12497.
(2) Rogelj, J.; Luderer, G.; Pietzcker, R. C.; Kriegler, E.; Schaeffer, M.; Krey, V.; Riahi, K. Energy system transformations for limiting end-of-century warming to below 1.5 degrees C. *Nat Clim Change* **2015**, *5* (6), 519-+. DOI: DOI 10.1038/nclimate2572.

(3) Boot-Handford, M. E.; Abanades, J. C.; Anthony, E. J.; Blunt, M. J.; Brandani, S.; Mac Dowell, N.; Fernandez, J. R.; Ferrari, M. C.; Gross, R.; Hallett, J. P.; et al. Carbon capture and storage update. *Energ Environ Sci* **2014**, *7* (1), 130-189. DOI: 10.1039/c3ee42350f.
(4) Med, N. A. S. E. Negative Emissions Technologies and Reliable Sequestration: A Research Agenda. *Negative Emissions Technologies and Reliable Sequestration: A Research Agenda* **2019**, 1-495. DOI: 10.17226/25259.
(5) Rosa, L.; Sanchez, D. L.; Mazzotti, M. Assessment of carbon dioxide removal potential via BECCS in a carbon-neutral Europe. *Energ Environ Sci* **2021**, *14* (5), 3086-3097. DOI: 10.1039/d1ee00642h.
(6) Jones, C. W. Metal-Organic Frameworks and Covalent Organic Frameworks: Emerging Advances and Applications. *Jacs Au* **2022**, *2* (7), 1504-1505. DOI: 10.1021/jacsau.2c00376.
(7) Sanz-Perez, E. S.; Murdock, C. R.; Didas, S. A.; Jones, C. W. Direct Capture of CO2 from Ambient Air. *Chem Rev* **2016**, *116* (19), 11840-11876. DOI: 10.1021/acs.chemrev.6b00173.
(8) Rim, G.; Kong, F. H.; Song, M. Y.; Rosu, C.; Priyadarshini, P.; Lively, R. P.; Jones, C. W. Sub-Ambient Temperature Direct Air Capture of CO2 using Amine-Impregnated MIL-101(Cr) Enables Ambient Temperature CO2 Recovery. *Jacs Au* **2022**, *2* (2), 380-393. DOI: 10.1021/jacsau.1c00414.
(9) Zhu, X. C.; Xie, W. W.; Wu, J. Y.; Miao, Y. H.; Xiang, C. J.; Chen, C. P.; Ge, B. Y.; Gan, Z. Z.; Yang, F.; Zhang, M.; et al. Recent advances in direct air capture by adsorption. *Chem Soc Rev* **2022**, *51* (15), 6574-6651. DOI: 10.1039/d1cs00970b.
(10) Heydari-Gorji, A.; Sayari, A. Thermal, Oxidative, and CO2-Induced Degradation of Supported Polyethylenimine Adsorbents. *Ind Eng Chem Res* **2012**, *51* (19), 6887-6894. DOI: 10.1021/ie3003446.
(11) Sayari, A.; Heydari-Gorji, A.; Yang, Y. CO2-Induced Degradation of Amine-Containing Adsorbents: Reaction Products and Pathways. *J Am Chem Soc* **2012**, *134* (33), 13834-13842. DOI: 10.1021/ja304888a.
(12) Didas, S. A.; Zhu, R. S.; Brunelli, N. A.; Sholl, D. S.; Jones, C. W. Thermal, Oxidative and CO2 Induced Degradation of Primary Amines Used for CO2 Capture: Effect of Alkyl Linker on Stability. *J Phys Chem C* **2014**, *118* (23), 12302-12311. DOI: 10.1021/jp5025137.
(13) Drage, T. C.; Arenillas, A.; Smith, K. M.; Snape, C. E. Thermal stability of polyethylenimine based carbon dioxide adsorbents and its influence on selection of regeneration strategies. *Micropor Mesopor Mat* **2008**, *116* (1-3), 504-512. DOI: 10.1016/j.micromeso.2008.05.009.
(14) Sakwa-Novak, M. A.; Jones, C. W. Steam Induced Structural Changes of a Poly(ethylenimine) Impregnated gamma-Alumina Sorbent for CO2 Extraction from Ambient Air. *Acs Appl Mater Inter* **2014**, *6* (12), 9245-9255. DOI: 10.1021/am501500q.
(15) Nezam, I.; Xie, J. W.; Golub, K. W.; Carneiro, J.; Olsen, K.; Ping, E. W.; Jones, C. W.; Sakwa-Novak, M. A. Chemical Kinetics of the Autoxidation of Poly(ethylenimine) in CO2 Sorbents. *Acs Sustain Chem Eng* **2021**, *9* (25), 8477-8486. DOI: 10.1021/acssuschemeng.1c01367.
(16) Racicot, J.; Li, S. C.; Clabaugh, A.; Hertz, C.; Akhade, S. A.; Ping, E. W.; Pang, S. H.; Sakwa-Novak, M. A. Volatile Products of the Autoxidation of Poly(ethylenimine) in CO2 Sorbents. *J Phys Chem C* **2022**, *126* (20), 8807-8816. DOI: 10.1021/acs.jpcc.1c09949.
(17) Carneiro, J. I., G.; Moon, H.J.; Guta, Y.; Proaño, L.; Sievers, C.; Sakwa-Novak, M.A.; Ping, E.P.; Jones, C.W. Insights into the Oxidative Degradation Mechanism of SolidAmine Sorbents for CO2 Capture from Air: Roles of Atmospheric Water. 2023.
(18) Bollini, P.; Choi, S.; Drese, J. H.; Jones, C. W. Oxidative Degradation of Aminosilica Adsorbents Relevant to Postcombustion CO2 Capture. *Energ Fuel* **2011**, *25* (5), 2416-2425. DOI: 10.1021/ef200140z.
(19) Sholl, D. S.; Lively, R. P. Exemplar Mixtures for Studying Complex Mixture Effects in Practical Chemical Separations. *Jacs Au* **2022**, *2* (2), 322-327. DOI: 10.1021/jacsau.1c00490.
(20) Barrett, E. P.; Joyner, L. G.; Halenda, P. P. The Determination of Pore Volume and Area Distributions in Porous Substances .1. Computations from Nitrogen Isotherms. *J Am Chem Soc* **1951**, *73* (1), 373-380. DOI: DOI 10.1021/ja01145a126.

(21) Kresse, G.; Furthmuller, J. Efficient iterative schemes for ab initio total-energy calculations using a plane-wave basis set. *Phys Rev B* **1996**, *54* (16), 11169-11186. DOI: DOI 10.1103/PhysRevB.54.11169.
(22) Blochl, P. E. Projector Augmented-Wave Method. *Phys Rev B* **1994**, *50* (24), 17953-17979. DOI: DOI 10.1103/PhysRevB.50.17953.
(23) Kresse, G.; Joubert, D. From ultrasoft pseudopotentials to the projector augmented-wave method. *Phys Rev B* **1999**, *59* (3), 1758-1775. DOI: DOI 10.1103/PhysRevB.59.1758.
(24) Perdew, J. P.; Burke, K.; Ernzerhof, M. Generalized gradient approximation made simple. *Phys Rev Lett* **1996**, *77* (18), 3865-3868. DOI: DOI 10.1103/PhysRevLett.77.3865.
(25) Grimme, S.; Antony, J.; Ehrlich, S.; Krieg, H. A consistent and accurate ab initio parametrization of density functional dispersion correction (DFT-D) for the 94 elements H-Pu. *J Chem Phys* **2010**, *132* (15). DOI: Artn 154104 Pmid 20423165 10.1063/1.3382344.
(26) Li, S. C.; Zheng, Y.; Gao, F.; Szanyi, J.; Schneider, W. F. Experimental and Computational Interrogation of Fast SCR Mechanism and Active Sites on H-Form SSZ-13. *Acs Catal* **2017**, *7* (8), 5087-5096. DOI: 10.1021/acscatal.7b01319.
(27) Colthup, N. B.; Daly, L. H.; Wiberley, S. E.; ProQuest. *Introduction to infrared and Raman spectroscopy*; Academic Press, 1990.
(28) Didas, S. A.; Salcwa-Novak, M. A.; Foo, G. S.; Sievers, C.; Jones, C. W. Effect of Amine Surface Coverage on the Co-Adsorption of CO2 and Water: Spectral Deconvolution of Adsorbed Species. *J Phys Chem Lett* **2014**, *5* (23), 4194-4200. DOI: 10.1021/jz502032c.
(29) Foo, G. S.; Lee, J. J.; Chen, C. H.; Hayes, S. E.; Sievers, C.; Jones, C. W. Elucidation of Surface Species through in Situ FTIR Spectroscopy of Carbon Dioxide Adsorption on Amine-Grafted SBA-15. *Chemsuschem* **2017**, *10* (1), 266-276. DOI: 10.1002/cssc.201600809.
(30) Ben Said, R.; Kolle, J. M.; Essalah, K.; Tangour, B.; Sayari, A. A Unified Approach to CO2-Amine Reaction Mechanisms. *Acs Omega* **2020**, *5* (40), 26125-26133. DOI: 10.1021/acsomega.0c03727.
(31) Yu, J.; Zhai, Y. X.; Chuang, S. S. C. Water Enhancement in CO2 Capture by Amines: An Insight into CO2-H2O Interactions on Amine Films and Sorbents. *Ind Eng Chem Res* **2018**, *57* (11), 4052-4062. DOI: 10.1021/acs.iecr.7b05114.
(32) Miller, D. D.; Yu, J.; Chuang, S. S. C. Unraveling the Structure and Binding Energy of Adsorbed CO2/H2O on Amine Sorbents. *J Phys Chem C* **2020**, *124* (45), 24677-24689. DOI: 10.1021/acs.jpcc.0c04942.
(33) Yu, J.; Chuang, S. S. C. The Structure of Adsorbed Species on Immobilized Amines in CO2 Capture: An in Situ IR Study. *Energ Fuel* **2016**, *30* (9), 7579-7587. DOI: 10.1021/acs.energyfuels.6b01423.
(34) Yu, J.; Chuang, S. S. C. The Role of Water in CO2 Capture by Amine. *Ind Eng Chem Res* **2017**, *56* (21), 6337-6347. DOI: 10.1021/acs.iecr.7b00715.
(35) Zhai, Y. X.; Chuang, S. S. C. The Nature of Adsorbed Carbon Dioxide on Immobilized Amines during Carbon Dioxide Capture from Air and Simulated Flue Gas. *Energy Technol-Ger* **2017**, *5* (3), 510-519. DOI: 10.1002/ente.201600685.
(36) Srikanth, C. S.; Chuang, S. S. C. Infrared Study of Strongly and Weakly Adsorbed CO2 on Fresh and Oxidatively Degraded Amine Sorbents. *J Phys Chem C* **2013**, *117* (18), 9196-9205. DOI: 10.1021/jp311232f.
(37) Tumuluri, U.; Isenberg, M.; Tan, C. S.; Chuang, S. S. C. In Situ Infrared Study of the Effect of Amine Density on the Nature of Adsorbed CO2 on Amine-Functionalized Solid Sorbents. *Langmuir* **2014**, *30* (25), 7405-7413. DOI: 10.1021/la501284y.
(38) Wilfong, W. C.; Srikanth, C. S.; Chuang, S. S. C. In Situ ATR and DRIFTS Studies of the Nature of Adsorbed CO2 on Tetraethylenepentamine Films. *Acs Appl Mater Inter* **2014**, *6* (16), 13617-13626. DOI: 10.1021/am5031006.
(39) Zhai, Y. X.; Chuang, S. S. C. Enhancing Degradation Resistance of Polyethylenimine for CO2 Capture with Cross-Linked Poly(vinyl alcohol). *Ind Eng Chem Res* **2017**, *56* (46), 13766-13775. DOI: 10.1021/acs.iecr.7b03636.

(40) Miller, D. D.; Chuang, S. S. C. Control of CO2 Adsorption and Desorption Using Polyethylene Glycol in a Tetraethylenepentamine Thin Film: An In Situ ATR and Theoretical Study. *J Phys Chem C* **2016**, *120* (44), 25489-25504. DOI: 10.1021/acs.jpcc.6b09506.
(41) Hedin, N.; Bacsik, Z. Perspectives on the adsorption of CO2 on amine-modified silica studied by infrared spectroscopy. *Curr Opin Green Sust* **2019**, *16*, 13-19. DOI: 10.1016/j.cogsc.2018.11.010.
(42) Hahn, M. W.; Jelic, J.; Berger, E.; Reuter, K.; Jentys, A.; Lercher, J. A. Role of Amine Functionality for CO2 Chemisorption on Silica. *J Phys Chem B* **2016**, *120* (8), 1988-1995. DOI: 10.1021/acs.jpcb.5b10012.
(43) Cendak, T.; Sequeira, L.; Sardo, M.; Valente, A.; Pinto, M. L.; Mafra, L. Detecting Proton Transfer in CO2 Species Chemisorbed on Amine-Modified Mesoporous Silicas by Using (CNMR)-C-13 Chemical Shift Anisotropy and Smart Control of Amine Surface Density. *Chem-Eur J* **2018**, *24* (40), 10136-10145. DOI: 10.1002/chem.201800930.
(44) Bacsik, Z.; Hedin, N. Effects of carbon dioxide captured from ambient air on the infrared spectra of supported amines. *Vib Spectrosc* **2016**, *87*, 215-221. DOI: 10.1016/j.vibspec.2016.10.006.
(45) Morsch, S.; Liu, Y. W.; Lyon, S. B.; Gibbon, S. R.; Gabriele, B.; Malanin, M.; Eichhorn, K. J. Examining the early stages of thermal oxidative degradation in epoxy-amine resins. *Polym Degrad Stabil* **2020**, *176*. DOI: ARTN 109147

10.1016/j.polymdegradstab.2020.109147.
(46) Srikanth, C. S.; Chuang, S. S. C. Spectroscopic Investigation into Oxidative Degradation of Silica-Supported Amine Sorbents for CO2 Capture. *Chemsuschem* **2012**, *5* (8), 1435-1442. DOI: 10.1002/cssc.201100662.
(47) Min, K.; Choi, W.; Kim, C.; Choi, M. Oxidation-stable amine-containing adsorbents for carbon dioxide capture. *Nat Commun* **2018**, *9*. DOI: ARTN 726

10.1038/s41467-018-03123-0.
(48) Li, S. C.; Ceron, M. R.; Eshelman, H. V.; Varni, A. J.; Maiti, A.; Akhade, S.; Pang, S. H. Probing the Kinetic Origin of Varying Oxidative Stability of Ethyl- vs. Propyl-spaced Amines for Direct Air Capture. *Chemsuschem* **2023**. DOI: 10.1002/cssc.202201908.
(49) Li, K. M.; Jiang, J. G.; Chen, X. J.; Gao, Y. C.; Yan, F.; Tian, S. C. Research on Urea Linkages Formation of Amine Functional Adsorbents During CO2 Capture Process: Two Key Factors Analysis, Temperature and Moisture. *J Phys Chem C* **2016**, *120* (45), 25892-25902. DOI: 10.1021/acs.jpcc.6b08788.
(50) Sayari, A.; Belmabkhout, Y. Stabilization of Amine-Containing CO2 Adsorbents: Dramatic Effect of Water Vapor. *J Am Chem Soc* **2010**, *132* (18), 6312-+. DOI: 10.1021/ja1013773.
(51) Zweifel, H.; Maier, R. D.; Schiller, M. *Plastics additives handbook*; Hanser Publications, 2009.
(52) Laio, A.; Parrinello, M. Escaping free-energy minima. *P Natl Acad Sci USA* **2002**, *99* (20), 12562-12566. DOI: 10.1073/pnas.202427399.
(53) Smith, L. M.; Aitken, H. M.; Coote, M. L. The Fate of the Peroxyl Radical in Autoxidation: How Does Polymer Degradation Really Occur? *Accounts Chem Res* **2018**, *51* (9), 2006-2013. DOI: 10.1021/acs.accounts.8b00250.
(54) Salahudeen, N.; Ahmed, A. S.; Al-Muhtaseb, A. H.; Dauda, M.; Waziri, S. M.; Jibril, B. Y. Synthesis of gamma alumina from Kankara kaolin using a novel technique. *Appl Clay Sci* **2015**, *105*, 170-177. DOI: 10.1016/j.clay.2014.11.041.
(55) Pang, S. H.; Lively, R. P.; Jones, C. W. Oxidatively-Stable Linear Poly(propylenimine)-Containing Adsorbents for CO2 Capture from Ultradilute Streams. *Chemsuschem* **2018**, *11* (15), 2628-2637. DOI: 10.1002/cssc.201800438.
(56) Vallace, A.; Brooks, S.; Coe, C.; Smith, M. A. Kinetic Model for CO2 Capture by Lithium Silicates. *J Phys Chem C* **2020**, *124* (37), 20506-20515. DOI: 10.1021/acs.jpcc.0c04230.
(57) Kwon, H. T.; Sakwa-Novak, M. A.; Pang, S. H.; Sujan, A. R.; Ping, E. W.; Jones, C. W. Aminopolymer-Impregnated Hierarchical Silica Structures: Unexpected Equivalent CO2 Uptake under Simulated Air

Capture and Flue Gas Capture Conditions. *Chem Mater* **2019**, *31* (14), 5229-5237. DOI: 10.1021/acs.chemmater.9b01474.